

---

---

## CASE REPORT

---

---

# Perineural and Muscular Involvement in Recurrent Diffuse Large B-Cell Lymphoma Detected by Fluorine-18 Fluorodeoxyglucose Positron Emission Tomography/Computed Tomography: A Case Report

JHY Lau, KK Ng, BT Kung

*Nuclear Medicine Unit, Department of Diagnostic and Interventional Radiology, Queen Elizabeth Hospital, Hong Kong SAR, China*

## CASE PRESENTATION

A 79-year-old female with a past medical history of hypertension and impaired fasting glucose presented to our institution in April 2020 with a neck mass and fever. She was an ex-smoker with no known drug allergies. Following an ear, nose, and throat consultation, she was diagnosed with stage 4B diffuse large B-cell lymphoma (DLBCL). A biopsy of the left tonsil revealed high-grade B-cell lymphoma, consistent with DLBCL. Further evaluation including bilateral bone marrow aspiration and bilateral trephine biopsy showed no evidence of lymphoma involvement.

Staging fluorine-18 fluorodeoxyglucose positron emission tomography/computed tomography (<sup>18</sup>F-FDG PET/CT) revealed hypermetabolic lymphadenopathy on both sides of the diaphragm, consistent with the biopsy-proven lymphoma, as well as hypermetabolic lesions in bilateral tonsils, confirming lymphomatous involvement (Figure 1).

The patient commenced R-CHOP chemotherapy (rituximab, cyclophosphamide, doxorubicin, vincristine, and prednisone), receiving six cycles over 5 months. The first cycle was administered at 50% dosage, with subsequent cycles adjusted for tolerance and side-effects. Following completion of the last cycle, an end-of-treatment <sup>18</sup>F-FDG PET/CT scan demonstrated complete metabolic remission, with a Deauville score of 2 (Figure 2).

Five months after completing R-CHOP chemotherapy, the patient developed a right neck mass and numbness over the right side of her neck and right lower limb, with muscle power graded at 2 out of 5. A CT scan revealed a large soft tissue mass on the right side of the oropharynx, and biopsy confirmed DLBCL with CD20 positivity. A subsequent <sup>18</sup>F-FDG PET/CT scan for restaging revealed a new hypermetabolic soft tissue mass in the right side of the oropharynx, consistent with lymphomatous involvement, with a Deauville score of 5. Notably,

---

---

*Correspondence: Dr JHY Lau, Nuclear Medicine Unit, Department of Diagnostic and Interventional Radiology, Queen Elizabeth Hospital, Hong Kong SAR, China*  
*Email: [hugh.lau@ha.org.hk](mailto:hugh.lau@ha.org.hk)*

Submitted: 16 December 2024; Accepted: 5 September 2025.

**Contributors:** All authors designed the study. JHYL acquired the data. All authors analysed the data. JHYL drafted the manuscript. KKN and BTK critically revised the manuscript for important intellectual content. All authors had full access to the data, contributed to the study, approved the final version for publication, and take responsibility for its accuracy and integrity.

**Conflicts of Interest:** All authors have disclosed no conflicts of interest.

**Funding/Support:** This study received no specific grant from any funding agency in the public, commercial, or not-for-profit sectors.

**Data Availability:** All data generated or analysed during the present study are available from the corresponding author on reasonable request.

**Ethics Approval:** This study was approved by the Central Institutional Review Board of Hospital Authority, Hong Kong (Ref No.: CIRB-2024-313-4). The requirement for patient consent was waived by the Board as the patient was deceased and no contact information for next of kin was available. The study involved retrospective review of anonymised clinical data only and posed no risk to subjects. All data were handled in accordance with Hospital Authority policies on data privacy and security.

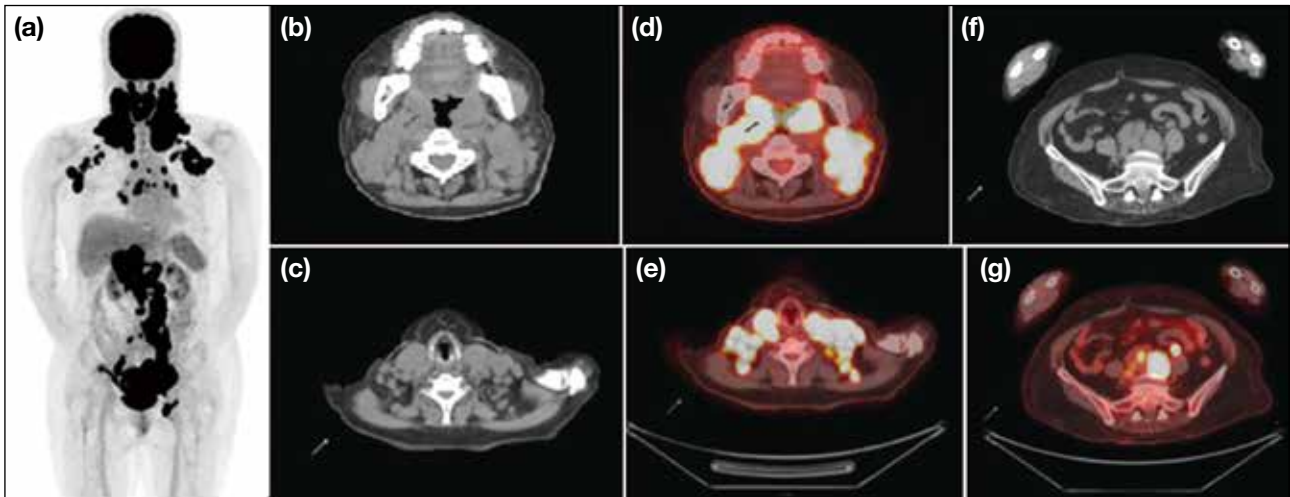


**Figure 1.** Staging fluorine-18 fluorodeoxyglucose positron emission tomography/computed tomography ( $^{18}\text{F}$ -FDG PET/CT) in a patient with biopsy-proven diffuse large B-cell lymphoma. (a) Maximum intensity projection shows multiple hypermetabolic, enlarged lymph nodes on both sides of the diaphragm. Transaxial (b and c) plain CT and (d and e) fused PET/CT images show supradiaphragmatic involvement, and transaxial (f) plain CT and (g) fused PET/CT images show infradiaphragmatic involvement.

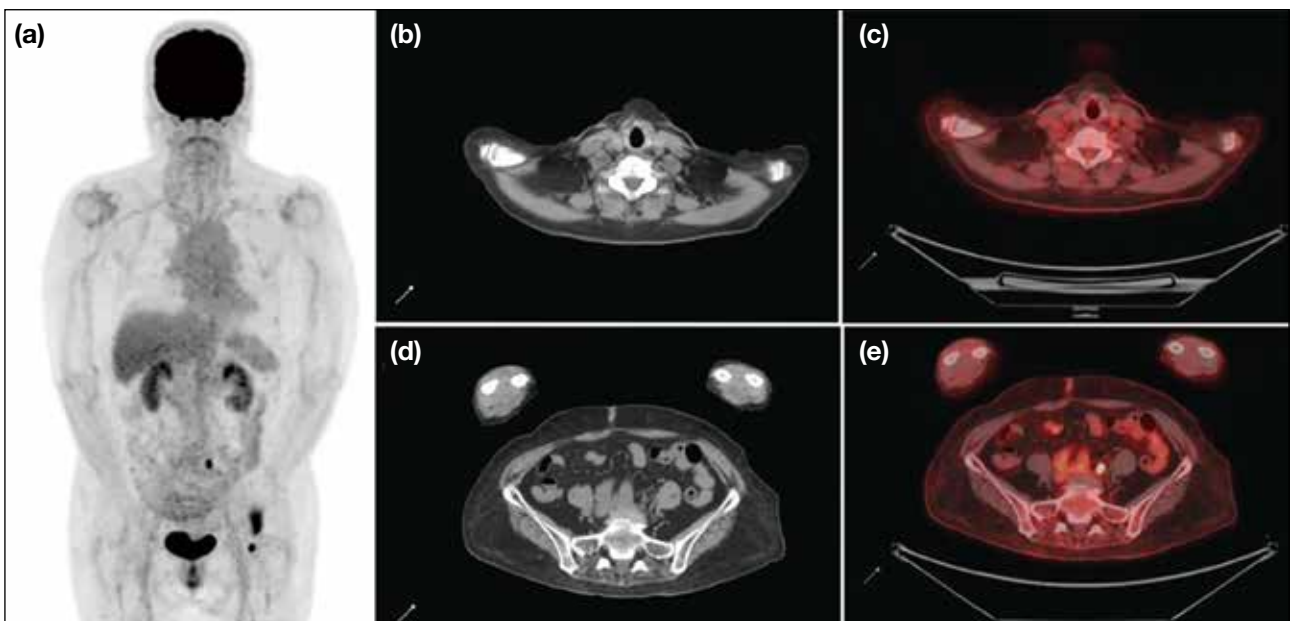


**Figure 2.** Fluorine-18 fluorodeoxyglucose positron emission tomography/computed tomography ( $^{18}\text{F}$ -FDG PET/CT) following treatment with R-CHOP chemotherapy (rituximab, cyclophosphamide, doxorubicin, vincristine, and prednisone). (a) Maximum intensity projection shows significant metabolic improvement or resolution on both sides of the diaphragm. Transaxial (b) plain CT and (c) fused PET/CT images show resolved supradiaphragmatic lymph nodes, and transaxial (d) plain CT and (e) fused PET/CT images show resolved infradiaphragmatic lymph nodes.

the scan also revealed new, multiple hypermetabolic foci involving perineural and muscular involvements in the bilateral head and neck regions and the right proximal lower limb, raising suspicion for perineural lymphomatous infiltration (Figure 3).

The patient subsequently received six cycles of

R-IMVP-16 (rituximab, ifosfamide, methotrexate, etoposide, and prednisone) over 5 months. End-of-treatment  $^{18}\text{F}$ -FDG PET/CT showed metabolic resolution of the right tonsillar/oropharyngeal mass and other infiltrative perineural lesions in the neck region and right lower limb, indicating a favourable treatment response (Figure 4). Clinically, her numbness subsided,

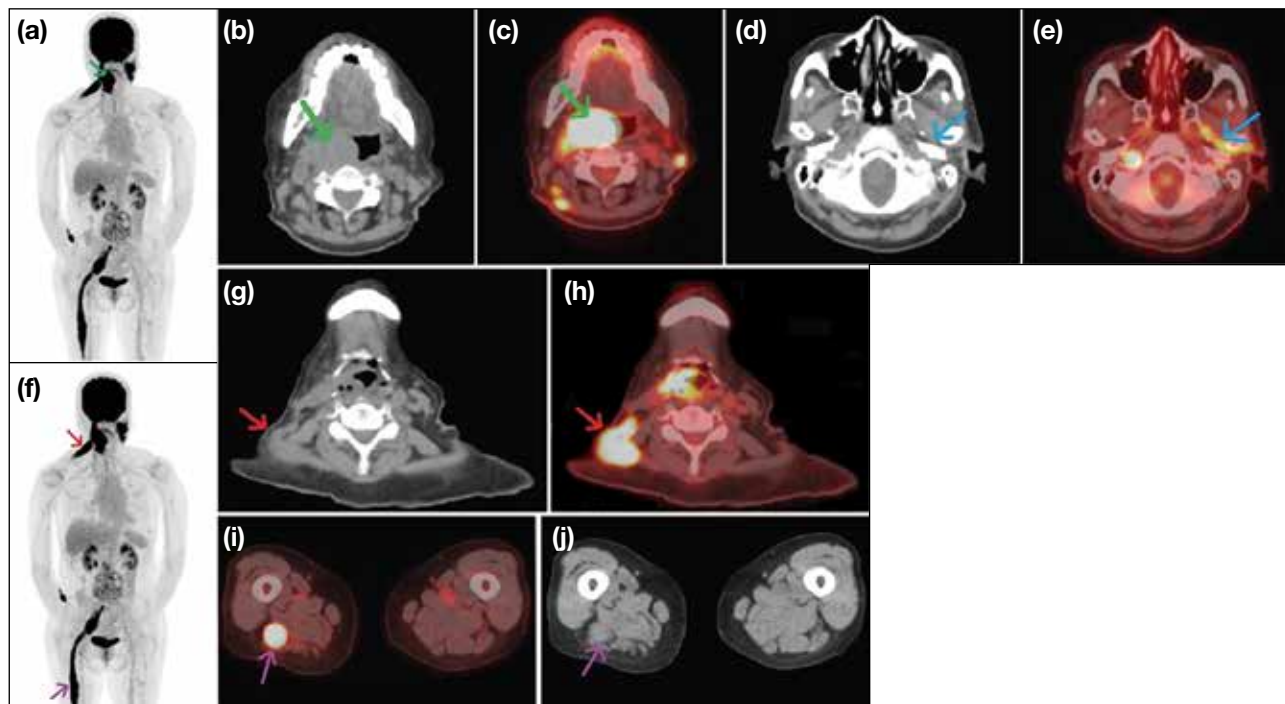


**Figure 3.** Recurrence and suspected atypical lymphomatous involvement in neuromuscular regions. (a) Maximum intensity projection of the fluorine-18 fluorodeoxyglucose positron emission tomography/computed tomography ( $^{18}\text{F}$ -FDG PET/CT) shows a hypermetabolic right oropharyngeal lesion (arrow). Transaxial (b) plain CT and (c) fused PET/CT images show the corresponding hypermetabolic lesion (arrows). Transaxial (d) plain CT and (e) fused PET/CT images show hypermetabolic left perineural involvement along the distribution of the left trigeminal branches (arrows). (f) Maximum intensity projection shows a hypermetabolic right neck perineural and muscular lesion (red arrow) and a right lower limb perineural and muscular lesion (purple arrow). Transaxial (g) plain CT and (h) fused PET/CT images show a hypermetabolic right neck neuromuscular lesion over the right trapezius muscle and accessory nerve region (arrows). Transaxial (i) plain CT and (j) fused PET/CT images show a hypermetabolic right lower limb neuromuscular lesion in the region of the right sciatic nerve (arrows).

with improved sensation in the previously affected regions and right lower limb power improved to 4 out of 5, consistent with the  $^{18}\text{F}$ -FDG PET/CT findings. Both clinical and imaging findings favoured a positive treatment response of the perineural and muscular lymphomatous involvement in this patient with recurrent lymphoma.

## DISCUSSION

Perineural and muscular involvement in DLBCL is rare, with only a limited number of cases reported in the literature.<sup>1</sup> The underlying mechanisms are not fully understood, but it is believed that DLBCL may infiltrate muscle tissue either via a haematogenous route or through adjacent lymphatic structures.<sup>2</sup> Clinical manifestations can vary widely, with patients presenting with muscle weakness, myalgia, or neuropathic symptoms.<sup>3</sup> Differential diagnoses for FDG-avid perineural and muscular lesions include polyneuritis, compartment-related compression radiculopathy, and tuberculosis. In polyneuritis, the pattern of increased FDG uptake is usually symmetrical and occurs without associated soft



**Figure 4.** Maximum intensity projection of fluorine-18 fluorodeoxyglucose positron emission tomography/computed tomography with significant metabolic improvements or resolutions of the oropharynx, right neck and right lower limb hypermetabolic lesions after treated with R-IMVP-16 (rituximab, ifosfamide, methotrexate, etoposide, and prednisone) chemotherapy.

tissue thickening.<sup>4,5</sup> The significant soft tissue thickening in our case made compartment-related compression radiculopathy less likely. Active tuberculosis was excluded through microbiological investigations.

This case demonstrated that the patient's neuropathic symptoms and imaging findings were indicative of perineural and muscular involvement. The identification of hypermetabolic activity in the muscles on <sup>18</sup>F-FDG PET/CT was crucial in establishing the diagnosis due to the asymmetrical metabolic distribution and soft tissue thickening in the affected regions. These abnormalities resolved in parallel with the biopsy-proven recurrent right oropharynx DLBCL, both metabolically and morphologically. Such findings are often mistaken for primary myopathies or neuropathies.

In our case, <sup>18</sup>F-FDG PET/CT not only confirmed the recurrence of DLBCL but also revealed the unusual sites of perineural and muscular involvement. This underscores the importance of considering extranodal manifestations of DLBCL, as it ultimately guided treatment decisions. Furthermore, the most recent <sup>18</sup>F-FDG PET/CT showed both metabolic and morphological resolution of the hypermetabolic perineural and muscular lesions, supporting the diagnosis of atypical lymphomatous involvement and reflecting a significant treatment response.

Previous studies<sup>6,7</sup> revealed that perineural and muscular involvement in DLBCL is largely underreported, with only a limited number of cases documented—primarily in patients with advanced-stage disease—and highlighted the importance of recognising <sup>18</sup>F-FDG PET/CT findings in atypical sites of lymphomatous involvement to avoid misdiagnosis and ensure appropriate management. Primary muscular lymphoma<sup>6</sup> and other atypical sites of DLBCL involvement<sup>6,7</sup> have also been reported.

The utility of <sup>18</sup>F-FDG PET/CT in the staging and treatment monitoring of DLBCL has been examined,<sup>8,9</sup> which concluded that this imaging modality provides valuable insights into disease burden and can identify sites of active disease that may not be evident on conventional imaging. This aligns with our case, in which <sup>18</sup>F-FDG PET/CT played a pivotal role in diagnosing perineural and muscular involvement in a one-stop-shop manner.

The management of DLBCL with perineural and muscular involvement is complex and often requires

a multidisciplinary approach.<sup>10,11</sup> Treatment options may include chemotherapy, radiotherapy, and targeted therapies, depending on the extent of disease and the patient's overall health.

In our case, the patient was commenced on a salvage chemotherapy regimen following relapse of DLBCL. Given the aggressive nature of her disease, close monitoring with repeat <sup>18</sup>F-FDG PET/CT was planned to assess treatment response. The prognosis for patients with perineural and muscular involvement in DLBCL varies, but early detection and timely intervention can significantly improve clinical outcomes.

## CONCLUSION

This case highlights the importance of <sup>18</sup>F-FDG PET/CT in detecting perineural and muscular involvement in patients with recurrent DLBCL. Early detection of the disease involvement using <sup>18</sup>F-FDG PET/CT can guide biopsy targeting, inform appropriate treatment strategies and serve as a reference for assessing treatment response on end-of-treatment imaging, all of which are crucial for improving patient outcomes.

## REFERENCES

1. Lim AT, Clucas D, Khoo C, Parameswaran BK, Lau E. Neurolymphomatosis: MRI and <sup>18</sup>F-FDG-PET features. *J Med Imaging Radiat Oncol*. 2016;60:92-5.
2. Murthy NK, Amrami KK, Broski SM, Johnston PB, Spinner RJ. Perineural spread of peripheral neurolymphomatosis to the cauda equina. *J Neurosurg Spine*. 2021;36:464-9.
3. Broski SM, Bou-Assaly W, Gross MD, Fig LM. Diffuse skeletal muscle F-18 fluorodeoxyglucose uptake in advanced primary muscle non-Hodgkin's lymphoma. *Clin Nucl Med*. 2009;34:251-3.
4. Xie X, Cheng B, Han X, Liu B. Findings of multiple neuritis on FDG PET/CT imaging. *Clin Nucl Med*. 2013;38:67-9.
5. Ankrah AO, Glaudemans AW, Maes A, Van de Wiele C, Dierckx RA, Vorster M, et al. Tuberculosis. *Semin Nucl Med*. 2018;48:108-30.
6. Iioka F, Tanabe H, Honjo G, Misaki T, Ohno H. Resolution of bone, cutaneous, and muscular involvement after haploidentical hematopoietic stem cell transplantation followed by post-transplant cyclophosphamide in adult T-cell leukemia/lymphoma. *Clin Case Rep*. 2020;8:1553-9.
7. Belmonte G, Caldarella C, Hohaus S, Manfredi R, Minordi LM. Muscle recurrence of a primarily nodal follicular lymphoma studied by contrast-enhanced <sup>18</sup>F-FDG PET/CT. *Clin Nucl Med*. 2020;45:65-7.
8. Kostakoglu L, Cheson BD. Current role of FDG PET/CT in lymphoma. *Eur J Nucl Med Mol Imaging*. 2014;41:1004-27.
9. Jing F, Liu Y, Zhao X, Wang N, Dai M, Chen X, et al. Baseline <sup>18</sup>F-FDG PET/CT radiomics for prognosis prediction in diffuse large B cell lymphoma. *EJNMMI Res*. 2023;13:92.
10. Adams HJ, Kwee TC. Prognostic value of interim FDG-PET in R-CHOP-treated diffuse large B-cell lymphoma: systematic review and meta-analysis. *Crit Rev Oncol Hematol*. 2016;106:55-63.
11. Wai SH, Lee ST, Cliffer ER, Bei M, Lee J, Hawkes EA, et al. Utility of FDG-PET in predicting the histology of relapsed or refractory lymphoma. *Blood Adv*. 2024;8:736-45.